Effects of Volatile Anesthetics versus Ketamine on Blood-Brain Barrier Permeability via Lipid-Mediated Alterations of Endothelial Cell Membranes

Behnam Noorani, Ekram Ahmed Chowdhury, Faleh Alqahtani, Yeseul Ahn, Ehsan Nozohouri, Sumaih Zoubi, Dhavalkumar Patel, Laurence Wood, Juyang Huang, Muhammad Bilal Siddique, Abraham Al-Ahmad, Reza Mehvar, and Ulrich Bickel

Department of Pharmaceutical Sciences (B.N., E.A.C., F.A., Y.A., E.N., S.Z., A.A.-A., U.B.), Center for Blood-Brain Barrier Research, (B.N., E.A.C., F.A., Y.A., E.N., S.Z., A.A.-A., R.M., U.B.), and LC-MS Core Facility (D.P.), Jerry H. Hodge School of Pharmacy, Texas Tech University Health Sciences Center, Amarillo, Texas; Department of Immunotherapy and Biotechnology, Jerry H. Hodge School of Pharmacy, Texas Tech University Health Sciences Center, Abilene, Texas (L.W.); Department of Physics and Astronomy, Texas Tech University, Lubbock, Texas (J.H., M.B.S.); Department of Pharmacology and Toxicology, College of Pharmacy, King Saud University, Riyadh, Saudi Arabia (F.A.); and Department of Biomedical and Pharmaceutical Sciences, Chapman University, School of Pharmacy, Irvine, California (R.M.)

Received April 20, 2022; accepted February 7, 2023

ABSTRACT

The purpose of this study was to investigate the effects of the volatile anesthetic agents isoflurane and sevoflurane, at clinically relevant concentrations, on the fluidity of lipid membranes and permeability of the blood-brain barrier (BBB). We analyzed the in vitro effects of isoflurane or ketamine using erythrocyte ghosts (sodium fluorescein permeability), monolayers of brain microvascular endothelial cells ([^{13}C]sucrose and fluorescein permeability), or liposomes (fluorescence anisotropy). Additionally, we determined the effects of 30-minute exposure of mice to isoflurane on the brain tight junction proteins. Finally, we investigated in vivo brain uptake of [^{13}C]mannitol and [^{13}C]sucrose after intravenous administration in mice under anesthesia with isoflurane, sevoflurane, or ketamine/xylazine in addition to the awake condition. Isoflurane at 1-mM and 5-mM concentrations increased fluorescein efflux from the erythrocyte ghosts in a concentration-dependent manner. Similarly, in endothelial cell monolayers exposed to 3% (v/v) isoflurane, permeability coefficients rose by about 25% for fluorescein and 40% for [^{13}C]sucrose, whereas transendothelial resistance and cell viability remained unaffected. Although isoflurane caused a significant decrease in liposomes

anisotropy values, ketamine/xylazine did not show any effects. Brain uptake clearance (apparent K_{in}) of the passive permeability markers in vivo in mice approximately doubled under isoflurane or sevoflurane anesthesia compared with either ketamine/xylazine anesthesia or the awake condition. In vivo exposure of mice to isoflurane did not change any of the brain tight junction proteins. Our data support membrane permeabilization rather than loosening of intercellular tight junctions as an underlying mechanism for increased permeability of the endothelial cell monolayers and the BBB in vivo.

SIGNIFICANCE STATEMENT

The blood-brain barrier controls the entry of endogenous substances and xenobiotics from the circulation into the central nervous system. Volatile anesthetic agents like isoflurane alter the lipid structure of cell membranes, transiently facilitating the brain uptake of otherwise poorly permeable, hydrophilic small molecules. Clinical implications may arise when potentially neurotoxic drugs gain enhanced access to the central nervous system under inhalational anesthetics.

Introduction

The blood-brain barrier (BBB) plays a fundamental role in preserving the function of the human brain (Hawkins and Davis, 2005). In diseases affecting the central nervous system, the integrity of the BBB is compromised (Zlokovic, 2008; Kadry et al., 2020). Additionally, the BBB may be affected by drug treatment, such as the reported BBB opening under general anesthesia with volatile agents (Tétrault et al., 2008;

ABBREVIATIONS: AUC, area under the curve; BBB, blood-brain barrier; BMEC, brain microvascular endothelial cell; Cbr, brain concentration; DiD, 1,1′-dioctadecyl-3,3,3′,3′-tetramethylindodicarbocyanine, 4-chlorobenzenesulfonate salt; DPH-PC, 2-(3-(diphenylhexatrienyl)propanoyl)-1-hexadecanoyl-sn-glycero-3-phosphocholine; DPPC, 1, 2-dipalmitoyl-sn-glycero-3-phosphocholine; EC, endothelial cell; EG, erythrocyte ghost; hBMEC, human brain-derived microvascular endothelial cell; ID, injected dose; iPSC, induced pluripotent stem cell; K_{in}, brain uptake clearance; NaFl, sodium fluorescein; PS, permeability surface area product; TEER, transendothelial electrical resistance; UPLC-MS/MS, ultra high performance liquid chromatography tandem mass spectrometry; ZO-1, Zona occludens 1.

Acharya et al., 2015). Approximately 60,000 patients experience general anesthesia daily in the United States alone (Brown et al., 2010). Postoperative confusion with a potential contribution to the development of dementia in elderly patients undergoing surgical procedures with general anesthesia has been discussed as early as 1955 (Bedford, 1955). Whether general anesthetic agents are themselves a causative factor in short-term postoperative cognition deficits is still controversial (Belrose and Noppens, 2019). Major surgery or lesions like head trauma trigger inflammatory responses that may compromise the BBB and result in postoperative cognitive decline (Terrando et al., 2010; Thal et al., 2012; Yang et al., 2017). Few studies investigated the effect of volatile anesthetics alone on the BBB without surgery. These studies reported an increase in BBB permeability under isoflurane (Tétrault et al., 2008) and structural changes to the BBB under both isoflurane and sevoflurane (Acharya et al., 2015).

Our understanding of the exact physicochemical nature and pharmacological relevance of the effects caused by inhalational anesthetics at clinical concentrations on cell membranes is still incomplete. We recently demonstrated that isoflurane at concentrations of 1 mM and 5 mM substantially decreased fluorescence anisotropies of 2-(3-(diphenylhexatrienyl)propanoyl)-1-hexadecanoyl-sn-glycero-3-phosphocholine (DPH-PC), Nile red, N,N,N-trimethyl-4-(6-phenyl-1,3,5-hexatrien-1-yl)-benzenaminium, and 4-methylbenzenesulfonae (TMA-DPH) in different membranes, indicating an increased membrane fluidity (Patel et al., 2020). Therefore, we put forward the hypothesis that increased BBB permeability caused by volatile anesthetics like isoflurane and sevoflurane is due to enhanced transmembrane diffusibility of otherwise restricted hydrophilic markers of barrier integrity. This was tested in permeability studies with sodium fluorescein (NaFl), sucrose, or mannitol in three experimental settings: 1) erythrocyte ghosts (EGs) loaded with NaFl, a simple in vitro system representing a physiologic lipid bilayer; 2) permeability measurements with NaFl and sucrose in an in vitro model of the BBB generated with monolayers of human brain-derived microvascular endothelial cells (hBMECs); and 3) pharmacokinetics and brain uptake studies of sucrose and mannitol in mice. For comparison, the in vivo experiments were performed in animals under ketamine/xylazine anesthesia, injectable agents chemically unrelated to isoflurane, and in unanesthetized (awake) mice. Anisotropy measurements with artificial lipid membranes in presence of ketamine/xylazine were also conducted and compared with measurements in presence of isoflurane.

Materials and Methods

Chemicals and Supplies. $[^{13}C_{12}]$sucrose, $[^{13}C_6]$sucrose, $[^2H_2]$sucrose, $[^{13}C_6]$mannitol and $[^2H_8]$mannitol was purchased from Omicron Biochemicals (South Bend, IN). The left superscript and right subscript numbers represent the isotope mass and the number of isotopes in each compound. Fluorescein sodium USP was purchased from Chem-Impex International (Wood Dale, IL). Liquid chromatography tandem mass spectrometry–grade solvents and analytical grade chemicals were obtained from reliable commercial sources. 1,2-dipalmitoyl-sn-glycero-3-phosphocholine (DPPC) was purchased from Avanti Polar Lipids (Alabaster, AL) and 2-(3-(diphenylhexatrienyl)propanoyl)-1-hexadecanoyl-sn-glycero-3-phosphocholine (DPH-PC) was obtained from Molecular Probes (Eugene, OR). Packed human red blood cells (RBCs) were obtained from the Oklahoma Blood Institute (Oklahoma City, OK).

Animals. Adult (2 to 3 months) male and female C57BL/6J mice were purchased from Jackson Laboratory (Bar Harbor, ME), and kept under controlled temperature and humidity conditions with free access to food and water. All animal procedures were approved by the Institutional Animal Care and Use Committee at Texas Tech University Health Sciences Center and complied with the National Research Council guidelines for care and use of animals. This manuscript adheres to the applicable ARRIVE guidelines. The total number of animals used in the experimental series reported here was 77. In four of these mice, the intravenous injection of the markers failed, and one mouse died under anesthesia before the terminal time point. All other animals ($n = 72$) were evaluated. Mice were randomly assigned to treatment groups or to different terminal time points in the experimental series.

Ultra High Performance Liquid Chromatography Tandem Mass Spectrometry–Based Analysis. Sample preparation steps and Ultra High Performance Liquid Chromatography Tandem Mass Spectrometry (UPLC-MS/MS)–based detection of the stable isotope-labeled sucrose and mannitol on a Nexera UPLC system (Shimadzu Scientific Instruments, Columbia, MD) with a QTRAP 5500 detector (SCIEX, Framingham, MA) were performed following our previously validated methods (Chowdhury et al., 2018; Noorani et al., 2020).

Fluorescence Anisotropy Measurements on Liposome Preparations. DPPC liposomes labeled with DPH-PC were prepared for steady state fluorescence anisotropy (r) measurements by the rapid solvent exchange method exactly as described (Patel et al., 2020) at a fluorescent probe:lipid ratio of 1:500. These liposome preparations were incubated in presence of either isoflurane or ketamine/xylazine. Fluorescence anisotropy (r) of DPH-PC was measured with a Photon Technology International (PTI) C61/2000 spectrofluorometer (Lawrenceville, NJ) using a T-mode single photon counting configuration as described (Patel et al., 2020). All of the measurements were done in quartz cuvettes with a micromagnetic stir bar at 37°C. The final volume of the liposomes, PBS, and aqueous isoflurane or ketamine/xylazine in the cuvette were kept at 3 ml. To establish stable initial values, we measured the anisotropy of DPH-PC five times. Then we added 0.75 ml of a saturated isoflurane solution, resulting in a final concentration of 5 mM, and measured the anisotropy five times during the first 10 minutes, followed by three more measurements at 15, 30, and 40 minutes. For anisotropy measurements with ketamine/xylazine, a stock solution containing 250 μg/ml ketamine and 25 μg/ml xylazine in PBS was prepared and added to the cuvettes with liposomes to achieve final concentrations of either 10 μg/ml ketamine and 1 μg/ml xylazine or 100 μg/ml ketamine and 10 μg/ml xylazine, respectively. A concentration of 10 μg/ml ketamine (equal to 36.5 μM) corresponds to the maximum initial plasma concentration observed in mice after i.p. injection of an anesthetic dose of 100 mg/kg ketamine HCl (Ganguly et al., 2018).

Effects of Isoflurane on Erythrocyte Ghosts. Erythrocyte ghosts (EGs) were prepared from red blood cells based on a published protocol (Doberstein et al., 1995) with minor modifications as described by us (Patel et al., 2020). The EGs were then resuspended in hypotonic buffer solution (5 mM NaPO$_4$, pH 7.5) with 0.02% sodium azide and stored at 4°C until further use. For loading with NaFl, the ghosts were incubated with 10 μM NaFl in the hypotonic buffer for 2 hours at 4°C, followed by addition of 10× PBS (1:9 vol/vol), incubation for 1 hour at 37°C, and centrifugation at 5000 g for 7 minutes. After discarding the supernatant, isotonic PBS-EDTA was added. Centrifugation and resuspension of the ghost pellet were repeated until the supernatant was clear. A separate batch of EGs was prepared by including 1,1′-dioctadecyl-3,3,3′,3′-tetramethylindodicarbocyanine, 4-chlorobenzenesulfonate salt (DiD) membrane dye during the NaFl loading process following the manufacturer's protocol. These dual-stained EGs were analyzed on an Amnis ImageStreamX Mk II imaging flow cytometer (Luminex, Seattle, WA) to visualize the internal loading with NaFl. The effect of isoflurane on single-labeled NaFl-loaded ghosts was assessed by directly adding a buffer solution, presaturated to 25 mM isoflurane (Patel et al., 2020), to the EG suspension to achieve final concentrations of 1 mM or 5 mM isoflurane, respectively. The preparations were used to fill a screw cap, Teflon-sealed, airtight Wheaton glass vial with 1 ml internal volume

(DWK Life Sciences, Millville, NJ). After sealing, the vials were incubated for 2 hours at 37°C in an incubator under gentle shaking. The EG in isoflurane-treated and control vials were centrifuged and resuspended in buffer before analysis by flow cytometry on a BD FACSVerse (Becton, Dickinson and Co., Franklin Lakes, NJ). The selection of the concentrations of isoflurane in these studies was based on previous in vitro studies by others (Akata et al., 2003). That report showed that a 1 mM isoflurane concentration in a protein-free physiologic salt solution corresponds to approximately 5% isoflurane in air and is considered to be an anesthetic concentration in vivo, taking into account the minimal alveolar concentrations and the blood:gas partition coefficient of this anesthetic gas.

In Vitro Permeability Study on Induced Pluripotent Stem Cell–Derived BBB Endothelial Cells. The human induced pluripotent stem cell line (iPSC; WiCell, Madison, WI) was used. IMR90-c4 were differentiated into brain microvascular endothelial cells (BMECs) following the established protocol (Lippmann et al., 2014; Nozohouri et al., 2021) and seeded on 24-well transwell inserts. After 48 hours, transendothelial electrical resistance (TEER) was obtained by averaging three measurements on each insert using a Millicell ERS electrode (Millipore, Bedford, MA), and permeability assays were performed as recently published (Noorani et al., 2020). In brief, the markers [$^{13}C_{12}$]sucrose (1 mg/ml) and NaFl (10 μM) were added to the apical, donor side of the insert. Isoflurane anesthesia was simulated in a hypoxia chamber placed in an incubator at 37°C. Isoflurane (3%) in nitrous oxide and oxygen (70/30 v/v) was bubbled at 0.5 l/min through a small water reservoir to humidify the chamber atmosphere. Achievement of 3% isoflurane in the chamber atmosphere was inferred when an oxygen sensor read 30% oxygen as in the supply line. Preincubation of the cells for 2 hours without isoflurane (baseline measurements) was followed by 6-hour exposure to isoflurane. Fifty-microliter aliquots were collected from the donor (blood side) and the acceptor (basolateral, brain side) compartments after the baseline and 6-hour isoflurane incubation periods. [$^{13}C_{12}$]sucrose concentrations were measured by UPLC-MS/MS and fluorescein concentrations were measured on a plate reader.

The clearance or permeability-surface area product (PS) for sucrose and NaFl was calculated as follows:

$$Cleared\ Volume = (C(acceptor)\ *V(acceptor))/C(donor) \tag{1}$$

where $C_{acceptor}$ refers to concentration in the acceptor compartment at a given sampling time point and $V_{acceptor}$ refers to the volume of the acceptor compartment. C_{donor} is the concentration in donor compartment. $C_{acceptor}$ is zero at time zero.

The PS was calculated as:

$$PS = (Cleared\ Volume)/(Sampling\ time) \tag{2}$$

The permeability coefficient (P) was calculated by dividing with the surface area (S) of the transwell insert:

$$P = PS/S \tag{3}$$

The permeability coefficient of the cell monolayer (P_{cells}) was obtained by correcting the total permeability (P_{total}) with the permeability coefficient of the coated filter alone (P_{blank}):

$$\frac{1}{P_{Cells}} = \frac{1}{P_{total}} - \frac{1}{P_{blank}} \tag{4}$$

BBB Permeability in Mice under Different Anesthesia Conditions. In the first experimental series, plasma kinetics and brain uptake of [$^{13}C_{12}$]sucrose were studied in mice anesthetized with either ketamine or isoflurane. Animals received isoflurane in 70% nitrous oxide/30% oxygen (3% for induction, 1.5%–2% for maintenance, applied via a silicone face mask at a flow rate of 1 l/min) or ketamine/xylazine (100:2 mg/kg) injected i.p. When required, a second, reduced dose of ketamine (50 mg/kg) was added after 60 minutes. Brain uptake was measured in groups of four mice at five terminal time points (15, 30, 60, 120, and 240 minutes). [$^{13}C_{12}$]sucrose (10 mg/kg in saline) was injected as an i.v. bolus dose in the left jugular vein, which was exposed by a small skin incision. Blood samples (30–50 μl) were drawn from the right jugular vein into heparinized 30-G insulin syringes. Thirty seconds before the terminal blood sample, mice received an i.v. bolus dose of [$^{13}C_6$]sucrose (10 mg/kg) as a vascular marker (Chowdhury et al., 2018). All animals were euthanized by decapitation immediately after the terminal blood sampling. Blood samples were centrifuged (5000 g, 10 minutes). Brains were rapidly removed from the skull, and forebrain (without olfactory bulb) was weighed and homogenized in 9 volumes of LC-MS/MS grade water. Plasma and brain samples were then frozen at -80°C until they were analyzed by UPLC-MS/MS.

In the second experimental series, we compared awake condition and different lengths (0.5, 2.5, and 3.5 hours) of anesthesia with isoflurane in nitrous oxide/oxygen (70/30 v/v) at 3% for induction and 1.5% for maintenance. Thirty minutes before each of these terminal sampling time points, 10 mg/kg [$^{13}C_{12}$]sucrose was injected via the jugular vein. Blood samples were collected at 1, 5, 10, 20, and 30 minutes during the last 30 minutes of the experiments from the right jugular veins of the anesthetized animals. For the awake group, different groups of mice were euthanized at each of the above times without undergoing anesthesia exposure. At 29.5 minutes, 10 mg/kg [$^{13}C_6$]sucrose was injected, and the terminal blood sample was drawn followed by brain sampling. Another group of mice was anesthetized for 3 hours with 1.5% isoflurane and allowed to wake up, and brain uptake of [$^{13}C_{12}$]sucrose was measured 24 hours later over 30 minutes under awake conditions using the method explained above for the awake group (different groups of animals for each sampling point).

In the third setting, BBB permeability of sucrose and mannitol was studied under four conditions: awake versus anesthesia with either isoflurane (3% for induction and 1.5%–2% v/v for maintenance) or sevoflurane (6% for induction and 2%–3% v/v for maintenance), both administered in 70% nitrous oxide/30% oxygen at a flow rate of 1 l/min via silicone face mask, or ketamine/xylazine cocktail (100:10 mg/kg) by i.p. injection. In the three anesthesia groups, [$^{13}C_{12}$]sucrose and [$^{13}C_6$]mannitol (10 mg/kg each) were coinjected as an i.v. bolus dose into the jugular vein. Blood samples (40 μl) were collected from the contralateral jugular vein at 1, 5, 10, 20, and 30 minutes. As above, [$^{13}C_6$]sucrose was injected as vascular marker before termination. In the awake group, the markers were injected via the tail vein and subgroups were decapitated after 1, 5, 15, or 30 minutes. The vascular marker, [$^{13}C_6$]sucrose, was only administered to the 30-minute group via tail vein injection at 29.5 minutes. Trunk blood after decapitation was collected in heparinized vials and centrifuged to obtain plasma. Plasma (from the 1-, 5-, 15-, and 30-minute subgroups) and brain samples (30-minute subgroup only) were analyzed by UPLC-MS/MS as described above.

All concentration values in plasma and brain were expressed as percent of injected dose per ml (% ID/ml), assuming that 1 g brain tissue corresponds to 1 ml.

Immunofluorescence Analysis of Tight Junction Proteins after Isoflurane Anesthesia in Mice. Animals received isoflurane in 70% nitrous oxide/30% oxygen with 10 minutes of induction (3%) and subsequent 30 minutes of maintenance (1.5%–2%) or stayed awake without any anesthesia ($n = 3$ per group). All animals were euthanized by cervical dislocation followed by decapitation. Brains were rapidly removed from the skull and snap-frozen in cryomolds with isopentane cooled in dry ice. Brains were stored at -80°C until cryosectioning on a Leica CM3050 cryostat. Forebrain coronal sections at 30 μm thickness containing the hippocampus were cut at a chamber temperature of -20°C. Sections were collected on Superfrost Plus slides and stored at -80°C until processing.

Cryosections were fixed for 10 minutes in 4% paraformaldehyde and subsequently rinsed three times in PBS. Sections were then permeabilized with 0.2% Triton X-100 containing 20 mM glycine in PBS for 1 hour at room temperature and washed three times with 0.2% Triton X-100 in PBS. Sections were blocked with 4% goat serum in PBS containing 0.2% Triton X-100 for 1 hour at room temperature before overnight incubation at 4°C with primary antibodies diluted in

4% goat serum and 0.2% Triton X-100. Primary antibodies used to label tight junction proteins were rabbit anti-claudin-5 IgG (1:500 final dilution; Cell Signaling #49564), rabbit anti-occludin IgG (1:100 final dilution; Cell Signaling #91131), and rabbit anti–Zona occludens 1 (ZO-1) IgG (1:100 final dilution; Invitrogen #40-2200). Sections were washed three times in 0.2% Triton X-100 and incubated in goat anti-rabbit secondary antibodies (1:500 final dilution; Invitrogen #A11008) for 1 hour at room temperature before three washes in PBS. Nuclei were counterstained with 4′,6-diamidino-2-phenylindole (DAPI) (300 nM) for 1 minute at room temperature before a final wash in PBS. Sections were cover-slipped with EMS-Mount Mounting Medium (EMS #17985-05) before imaging. Images were taken on a Leica Stellaris 8 confocal microscope with a 20× oil objective. Images were analyzed in Aivia (Leica Microsystems) by thresholding and segmenting the fluorescent signal from the background. The mean intensity of the segmented microvessels labeled with tight junction proteins was obtained, and an average of the mean intensities for an entire image was calculated. Four to five randomly chosen fields from two cortex and two hippocampus sections were analyzed per animal. Unpaired t tests were performed between the isoflurane-treated group and the awake control group.

Pharmacokinetic Analysis. The corrected brain concentration was calculated as follows:

$$C_{br-\text{corr}}^{analyte} = \frac{(V_d - V_0) \times C_{pl}^{analyte}}{1 - V_0} \qquad (5)$$

Here, V_d is the apparent volume of distribution of the BBB permeability marker [$^{13}C_6$]mannitol or [$^{13}C_{12}$] sucrose in the brain, V_0 is the apparent brain volume of distribution of the vascular marker [$^{13}C_6$] sucrose, and $C_{pl}^{analyte}$ is the terminal plasma concentration of [$^{13}C_6$]mannitol or [$^{13}C_{12}$]sucrose. These values were obtained by the following equations:

$$V_d = C_{br}^{analyte} / C_{pl}^{analyte} \qquad (6)$$

$$V_0 = C_{br}^{vascular\,marker} / C_{pl}^{vascular\,marker} \qquad (7)$$

where $C_{br}^{analyte}$ is the total uncorrected brain concentration of [$^{13}C_6$]mannitol or [$^{13}C_{12}$]sucrose, $C_{br}^{vascular\,marker}$ is the total uncorrected brain concentration of [$^{13}C_6$]sucrose at the terminal sampling time, and $C_{pl}^{vascular\,marker}$ is the terminal plasma concentration of the vascular marker.

The apparent brain uptake clearance, K_{in} (equivalent to PS) was calculated as follows:

$$K_{in} = C_{br-\text{corr}}^{analyte} / AUC_0^T \qquad (8)$$

AUC_0^T denotes the area under the plasma concentration-time curve from time 0 to the terminal sampling time. AUC_0^T was estimated via the logarithmic trapezoidal method. For those mice with serial blood sampling, individual area under the curve (AUC) values were calculated.

To compare the brain concentrations in the first experimental series (15 minutes to 240 minutes), we calculated the AUC according to Bailer's method (Bailer, 1988).

Statistical Analysis. We performed power analysis in STATA/MP 17.0 (StataCorp, College Station, TX). In a previous study in transwells, the relative standard deviation of permeability measurements was 0.06 (Noorani et al., 2020). For the in vitro studies, we considered a mean difference of at least 20% between groups as biologically relevant. With alpha = 0.05, a sample size of $n = 5$ gives 90% power to detect a difference of >14%. For the in vivo studies, with a relative standard deviation of 0.16 for apparent K_{in} (from pilot studies in awake mice) and alpha = 0.05, a sample size of at least $n = 4$ gives 90% power to detect a mean group difference of >44% from control (awake condition). We considered a difference of at least 50% in the K_{in} value (the primary parameter of interest for the in vivo studies) as biologically relevant.

For both in vitro and in vivo studies, the analytical assays were performed by investigators unaware of sample identities.

Prism 9.3 (GraphPad Software, La Jolla, CA) was used for all graphing and statistical analysis. Data are presented as individual values, means, and 95% confidence intervals (CIs). A P value < 0.05 was considered statistically significant. Comparisons of three or more groups were analyzed by one-way ANOVA followed by Tukey's multiple-comparison test. When comparing data from two groups, the two-sided t test was applied. To control P values for multiple t tests, the false discovery rate approach (FDR, with a desired value of 1%) with the two-stage step-up method of Benjamini, Krieger, and Yekutieli was used, and the adjusted q-values are reported. The Z test was applied to compare the AUCs in brain.

Results

Permeability of Erythrocyte Ghosts. NaFl-loaded EGs were stable for at least 7 days at 4°C and for at least 8 hours at 37°C as confirmed by constant fluorescence intensity on flow cytometry. Ghosts colabeled with DiD gave the expected images depicting a central green signal surrounded by red membrane staining (Fig. 1A). When single labeled, NaFl-loaded EGs, which were exposed for 2 hours to isoflurane, showed a loss in mean NaFl fluorescence intensity by 14% at 1 mM and 22% at 5 mM, indicating that the increased membrane fluidity caused by isoflurane is accompanied by concentration-dependent enhanced membrane permeability for low molecular weight hydrophilic molecules (Fig. 1, B and C).

Isoflurane Effect on iPSC-derived BBB Endothelial Cells. The mean (95% CI) permeability (cm/min) of BMECs exposed to 3% isoflurane in nitrous oxide/oxygen was increased compared with controls (Fig. 2A) from 4.03×10^{-5} [$3.41 \times 10^{-5} - 4.66 \times 10^{-5}$] to 5.01×10^{-5} [$4.70 \times 10^{-5} - 5.33 \times 10^{-5}$] ($P = 0.0046$) for fluorescein and from 3.59×10^{-5} [$2.77 \times 10^{-5} - 4.42 \times 10^{-5}$] to 5.06×10^{-5} [$2.77 \times 10^{-5} - 4.42 \times 10^{-5}$] ($P = 0.0019$) for [$^{13}C_{12}$] sucrose. However, TEER values were not affected (Fig. 2B), and the 3-(4,5-Dimethylthiazol-2-yl)-2,5-Diphenyltetrazolium Bromide (MTT) assay did not reveal any degree of cytotoxicity over the duration of the experiment (Fig. 2C).

Fluorescence Anisotropy of DPPC Lipid Membranes in Presence of Isoflurane or Ketamine/Xylazine. As shown in Fig. 3, isoflurane (5 mM) resulted in a significant decrease of DPH-PC anisotropy, which is in line with our previously published data on increased membrane fluidity under this agent (Patel et al., 2020). In contrast, the injectable anesthetic ketamine/xylazine had no effect on DPH-PC anisotropy values at a concentration corresponding to peak plasma concentrations reported in mice receiving a dose of 100 mg/kg ketamine HCl by i.p. administration (Ganguly et al., 2018) or at a 10-fold higher concentration.

Brain Uptake of [$^{13}C_{12}$]Sucrose in Mice under Ketamine/Xylazine or Isoflurane Anesthesia. The plasma concentration-time profiles of [$^{13}C_{12}$]sucrose were similar for both isoflurane and ketamine/xylazine anesthesia methods in five separate experimental groups when the sampling was conducted for 15 (Fig. 4A), 30 (Fig. 4B), 60 (Fig. 4C), 120 (Fig. 4D), or 240 (Fig. 4E) minutes. Additionally, there were no significant differences in the plasma AUCs of [$^{13}C_{12}$]sucrose between the two anesthesia methods for any of the five experiments (Fig. 4F). In contrast, brain concentrations were higher under isoflurane than ketamine anesthesia (Fig. 4G), which resulted in a 54% increase ($P < 0.0001$) in the brain AUC (Fig. 4H). Importantly, apparent brain uptake clearance (K_{in}) of [$^{13}C_{12}$]sucrose was
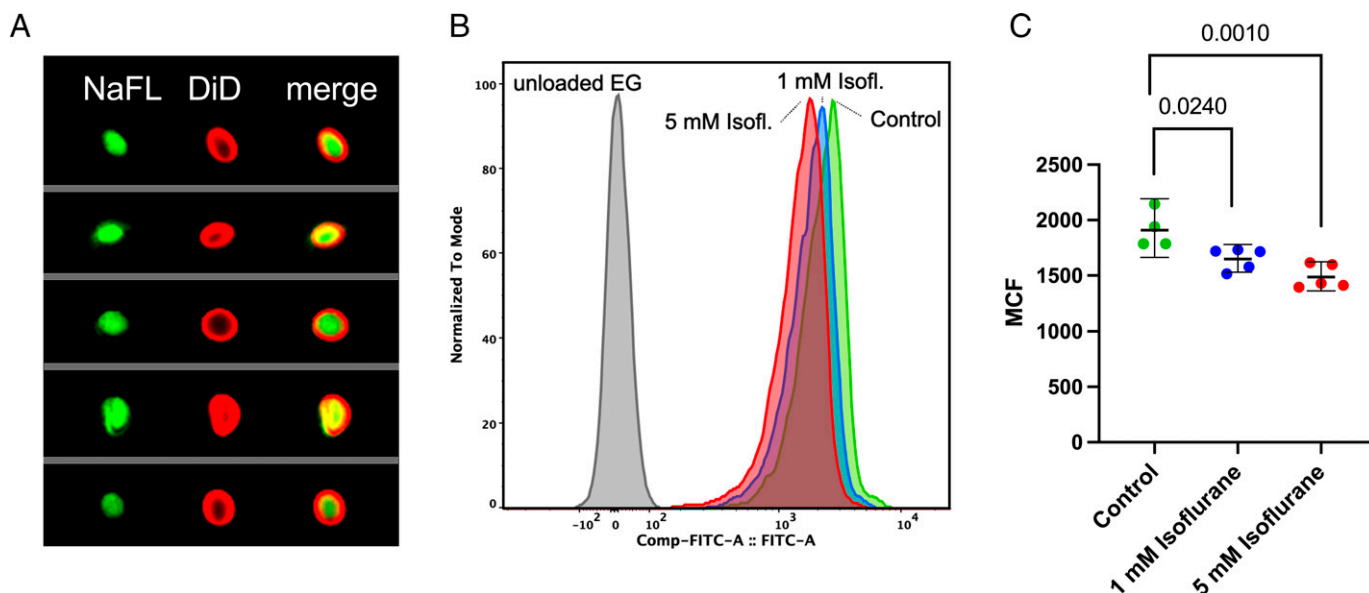
Fig. 1. Imaging flow cytometry of dual labeled erythrocyte ghosts shows internally loaded NaFl- and DiD-labeled membrane (A). Flow cytometry data of NaFl-loaded EG in (B) illustrate concentration-dependent loss of mean channel fluorescence (MCF) after incubation with 1 mM or 5 mM isoflurane for 2 hours compared with buffer control, as plotted in (C), with mean and CI. One-way ANOVA, $P = 0.0013$ ($n = 3$ for control, $n = 4$ for 1 mM and 5 mM); P values for individual group comparisons by Tukey's post-test are given in (C).

higher under isoflurane anesthesia at all sampling time points (Fig. 4I). The highest absolute and relative increase in apparent K_{in} occurred at 30 minutes, with a factor of 2 [0.129 (0.091–0.168) $\mu l \cdot min^{-1} \cdot g^{-1}$ for isoflurane vs. 0.0661 (0.0411–0.0911) $\mu l \cdot min^{-1} \cdot g^{-1}$ for ketamine (q = 0.0084)]. When plasma concentrations have declined more from the initial maximum, the assumption of unidirectional uptake no longer holds and efflux from brain tissue has increasing impact, explaining lower apparent K_{in} values at later sampling times.

Time and Concentration Dependence of the Isoflurane Effect. In this experiment, animals were naïve (awake) or kept under isoflurane for different periods before injection of the marker. As shown in Fig. 5, apparent K_{in} ($\mu l \cdot min^{-1} \cdot g^{-1}$) under 1.5% isoflurane for 0.5 hours doubled compared with awake mice [0.129 (0.091–0.168) vs. 0.0695 (0.0568–0.0822), $P = 0.026$] and increased further under 2.5 hours or 3.5 hours of anesthesia without reaching statistical significance compared with 0.5 hours. The effect appears fully reversible because 24 hours after 3 hours of isoflurane anesthesia, the BBB permeability is not different from naïve animals (Fig. 5).

Different isoflurane maintenance concentrations over 30 minutes revealed concentration-dependent increases in the apparent K_{in} of [$^{13}C_{12}$]sucrose (Fig. 5), which went from 0.129 (0.091–0.168) at 1.5% to 0.197 (0.143–0.168) $\mu l \cdot min^{-1} \cdot g^{-1}$ at 3% isoflurane ($P = 0.022$).

BBB Permeability in Awake Mice and under Ketamine, Isoflurane, or Sevoflurane Anesthesia. Figure 6 illustrates the plasma, brain, and apparent K_{in} data for sucrose (left panels) and mannitol (right panels). The plasma profiles of all treatment conditions were similar for both markers, sucrose and mannitol, with an apparent multiexponential decline (see Fig. 6, A and E). Correspondingly, the AUC values from 0 to 30 minutes were comparable, with sevoflurane being somewhat lower (Fig. 6, B and F).

The brain concentrations of mannitol were 1.8- to 2-fold higher than the corresponding sucrose concentrations under all treatment conditions (Fig. 6, C and G). Although the brain concentrations

(C_{br}) of the markers were similar in the awake and ketamine groups, the concentrations in the volatile anesthetic groups were higher than either awake or ketamine groups. For instance, C_{br} (% ID/ml) values of sucrose were 0.0213 (0.0160–0.0266) and 0.0166 (0.0134–0.0197) for the awake and ketamine groups, respectively, whereas C_{br} values of sucrose were 0.0315 (0.0251–0.0378) and 0.0357 (0.0315–0.0399) for the sevoflurane and isoflurane groups, respectively (Fig. 6C). Similarly, C_{br} (% ID/ml) values of mannitol were 0.0436 (0.0362–0.0510) and 0.0365 (0.0283–0.0446) for the awake and ketamine groups, respectively, whereas C_{br} values of mannitol were 0.0580 (0.0444–0.0716) and 0.0715 (0.0635–0.0796) for the sevoflurane and isoflurane groups, respectively (Fig. 6G).

Similarly, apparent K_{in} values were different between the volatile anesthetic groups (sevoflurane and isoflurane) and ketamine or awake groups (Fig. 6, D and H): K_{in} values of sucrose ($\mu l \cdot min^{-1} \cdot g^{-1}$) (Fig. 6D) were 0.0669 (0.0501–0.0836) and 0.0612 (0.0463–0.0760) for the awake and ketamine groups, respectively ($P = 0.96$ ketamine vs. awake), whereas K_{in} value of sucrose for the sevoflurane group was 0.144 (0.126–0.163) ($P = 0.005$ sevoflurane vs. awake and $P < 0.0001$ sevoflurane vs. ketamine). K_{in} value ($\mu l \cdot min^{-1} \cdot g^{-1}$) of sucrose for the isoflurane group was 0.126 (0.0991–0.153) ($P = 0.0005$ isoflurane vs. awake and $P = 0.0001$ isoflurane vs. ketamine). K_{in} values of mannitol ($\mu l \cdot min^{-1} \cdot g^{-1}$) (Fig. 6H) were 0.141 (0.117–0.165) and 0.153 (0.136–0.170) for the awake and ketamine groups, respectively, whereas K_{in} values of mannitol were 0.262 (0.218–0.306) and 0.268 (0.245–0.290) for the sevoflurane and isoflurane groups, respectively. Comparisons between the sevoflurane and either the awake or ketamine group gave P values less than 0.0001, and the same was the case for comparisons of isoflurane to either the awake or ketamine group. It is obvious that the apparent K_{in} value of mannitol is about twice as high as that of sucrose and that the increases in K_{in} caused by sevoflurane and isoflurane are comparable for both markers (Fig. 6, D and H).
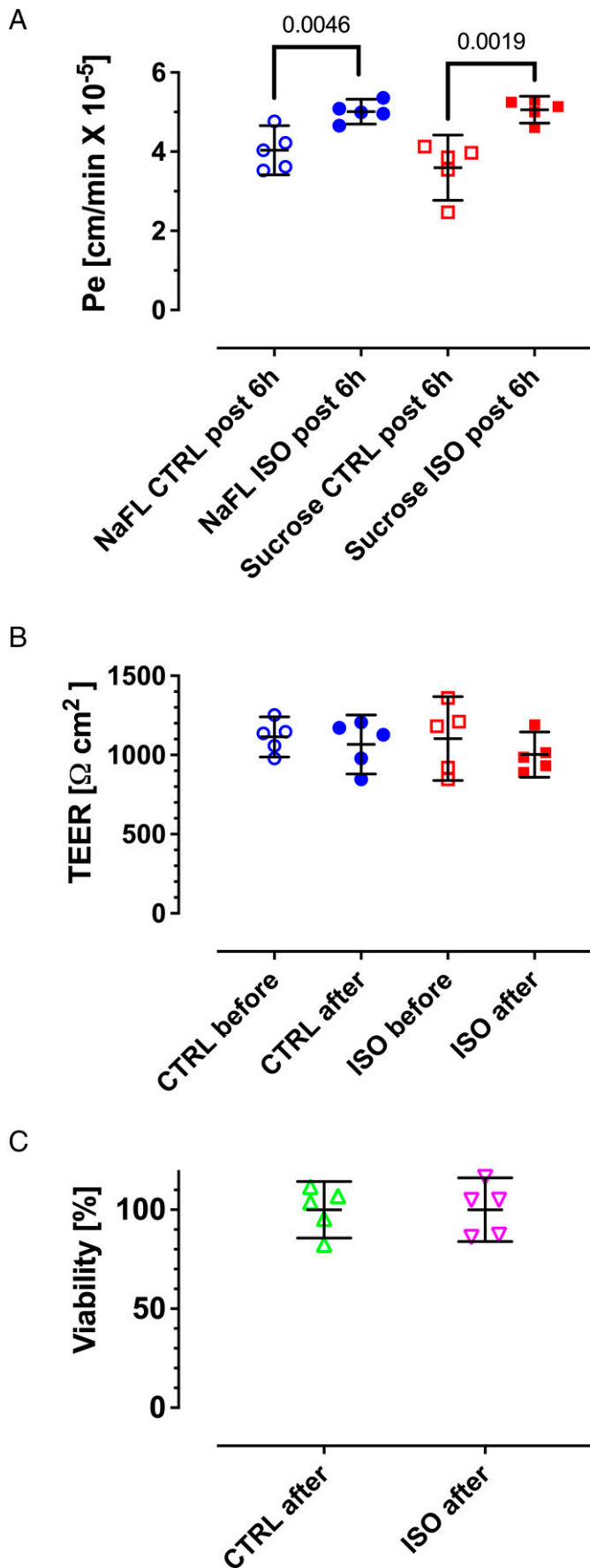
A

B

C
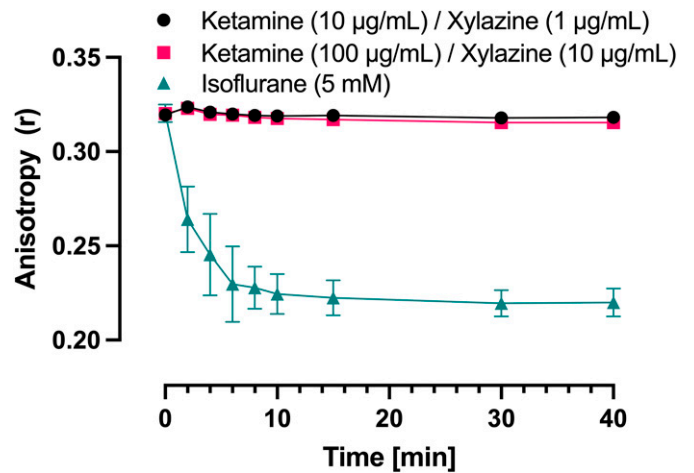
Fig. 3. DPH-PC fluorescence anisotropy measurements in DPPC liposomes after addition at time 0 of either 5 mM isoflurane (blue) or ketamine:xylazine at 10 μg/ml:1 μg/ml (black) or 100 μg/ml:10 μg/ml (red). Mean ± S.D. of three technical replicates. For some of the data points the standard deviation is smaller than the width of the symbols.

Ex Vivo Quantitative Immunofluorescence Analysis of Tight Junction Proteins after Isoflurane Anesthesia. To determine whether the increased BBB permeability in vivo, evident after even a brief exposure to isoflurane anesthesia, correlates with changes in the tight junction protein expression of brain microvascular endothelial cells, we quantified the immunofluorescence signals of claudin-5, occludin, and ZO-1 on brain sections. We compared a control group of naïve, unanesthetized mice with animals kept for 30 minutes under 1.5% isoflurane in nitrous oxide/oxygen (70%/30%) after induction with 3% isoflurane. Figure 7 illustrates that neither of the three proteins showed a statistically significant difference between control and isoflurane groups.

Discussion

Our results are compatible with the following conclusions. 1) At clinically relevant concentrations, isoflurane enhances the permeability of erythrocyte cell membranes to hydrophilic small molecules. 2) Isoflurane makes monolayers of iPSC-derived BMECs more permeable. 3) Short-term (30-minute) isoflurane and sevoflurane anesthesia increases BBB permeability in vivo about 2-fold, whereas ketamine/xylazine anesthesia yields K_{in} values similar to awake mice. The latter is consistent with unaffected fluorescence anisotropy values of liposome preparations in presence of ketamine/xylazine. 4) The isoflurane effect in vivo increases slightly with higher inhaled concentration or longer exposure, but it is fully reversible. 5) Enhanced BBB permeability under short-term isoflurane anesthesia is not accompanied by a detectable decrease in tight junction protein expression in brain capillaries.

**Fig. 2.** (A) iPSC-derived brain endothelial monolayers in transwells were preincubated at 37°C for 2 hours. NaFl or [13C12]sucrose was then added to the apical compartment, and permeability (Pe) across the monolayer was measured over 6 hours of incubation under 3% isoflurane (ISO) in nitrous oxide/oxygen (70/30) or under control conditions without isoflurane (CTRL). P values from unpaired two-sided t test, $n = 5$. (B) TEER values were measured before and after the 6-hour incubation period under control conditions (CTRL before, CTRL after) or isoflurane (ISO before, ISO after) and were found unchanged. (C) Viability measured by 3-(4,5-Dimethylthiazol-2-yl)-2,5-Diphenyltetrazolium Bromide (MTT) assay of isoflurane-treated cells assay after incubation (ISO after) matched viability of controls (CTRL after). All graphs depict individual values, means, and CI.
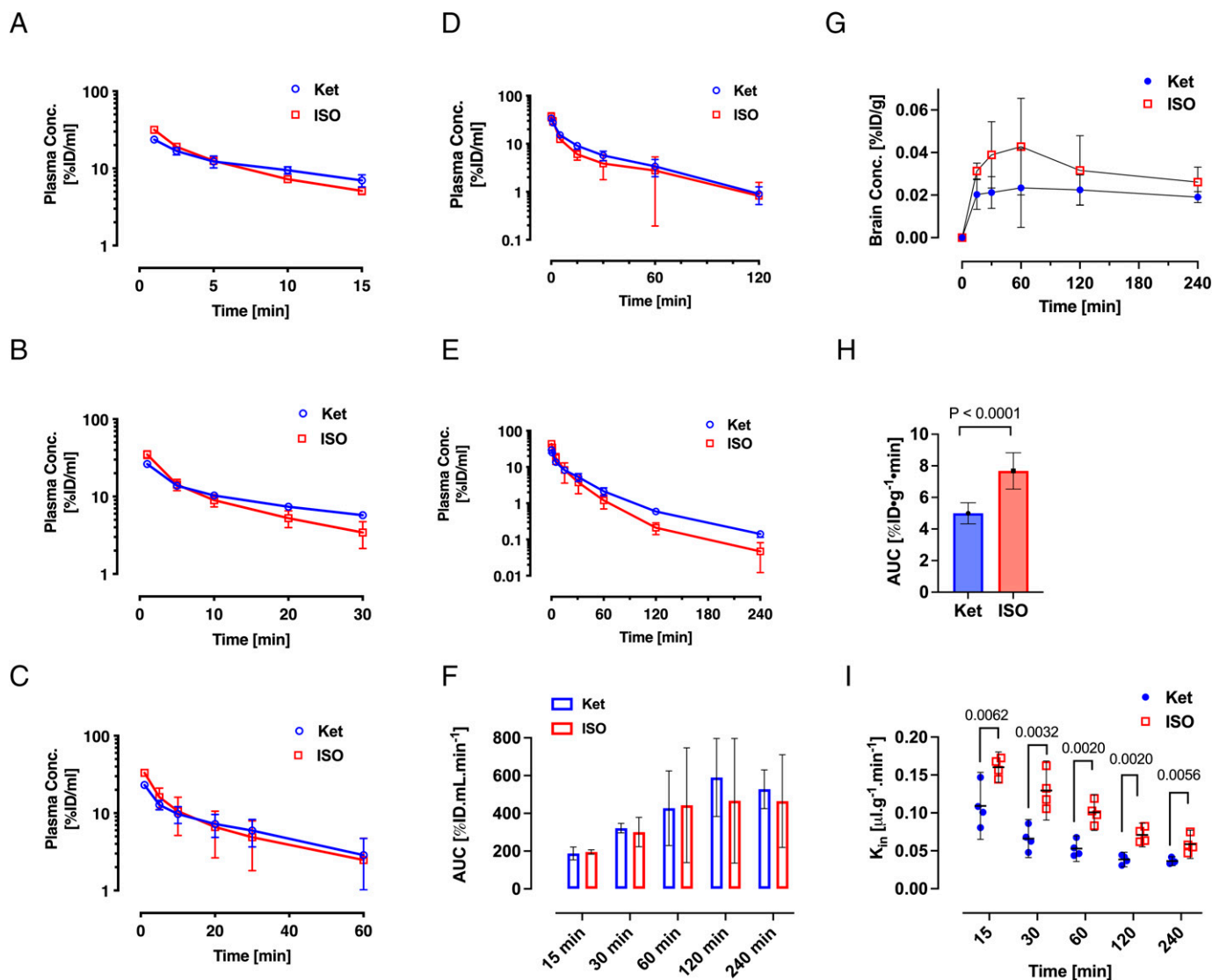
Fig. 4. Plasma profiles after intravenous bolus injection of [13C12]sucrose at time 0 in mice anesthetized with ketamine/xylazine (Ket) or isoflurane (ISO) in five separate experimental groups with terminal time points of 15, 30, 60, 120, or 240 minutes for brain sampling (panels A–E, mean and CI). In all mice, repeated blood samples were drawn from the jugular vein up to the terminal time point. Panel (F) depicts the area under the curve (AUC) in plasma (mean and CI). The concentration–time course of [13C12]sucrose in brain is depicted in (G) (mean and CI), and the AUC in brain from 0 to 240 minutes is shown in (H) (mean and CI). Panel (I) demonstrates apparent brain uptake clearance (K_{in}) of [13C12]sucrose under isoflurane and ketamine/xylazine anesthesia. Multiple unpaired two-sided t tests at each time point (in F and I) were adjusted for a 1% false discovery rate (FDR); $n = 4$ for all groups.

The present study extends our recent findings of increased membrane fluidity in artificial and natural lipid membranes under isoflurane (Patel et al., 2020). Anesthesia with this agent, and with the physicochemically related sevoflurane, which is now preferred clinically, induces a temporary increase in BBB permeability in vivo, which can be quantified by small molecular weight, hydrophilic markers like sucrose, mannitol, and the fluorescent dye NaFl. It is generally assumed that organ uptake of these so-called "paracellular" markers reflects leakiness between adjacent microvascular endothelial cells. Physiologically, paracellular diffusion at the BBB is highly restricted by complex tight junctions and adherens junctions. However, these markers have a low, yet measurable, lipid solubility: The octanol:water partition coefficients, log P, of sucrose and mannitol are −2.98 ± 0.033 and −3.62 ± 0.056, respectively (Noorani et al., 2020). Different mechanisms have been proposed to explain increased BBB permeability under volatile anesthetics. One potential mechanism is reduction

of tight junction integrity. Some studies claim evidence for that, although most were conducted in the context of concomitant brain injury (Thal et al., 2012) or major surgical procedures (Yang et al., 2017). For example, Thal et al. (2012) described a loss of tight junction protein ZO-1 in mice subject to experimental traumatic brain injury and isoflurane anesthesia but not in naïve animals after isoflurane exposure. Yang et al. (2017) saw decreased levels of claudin-1, ZO-1, and occludin in mice undergoing laparotomy under isoflurane anesthesia. Acharya et al. (2015) described enhanced leakage of endogenous IgG into the brain of rats undergoing 3 hours of anesthesia with sevoflurane or isoflurane, as detected by immunohistochemistry, and endothelial cell damage in scanning electron microscopic images, alterations in tight junctional folds, and even occasional death of endothelial cells. In contrast, a recent study by Saher's group could not confirm alterations of tight junction protein expression in mouse brain under isoflurane (Spieth et al., 2021). In
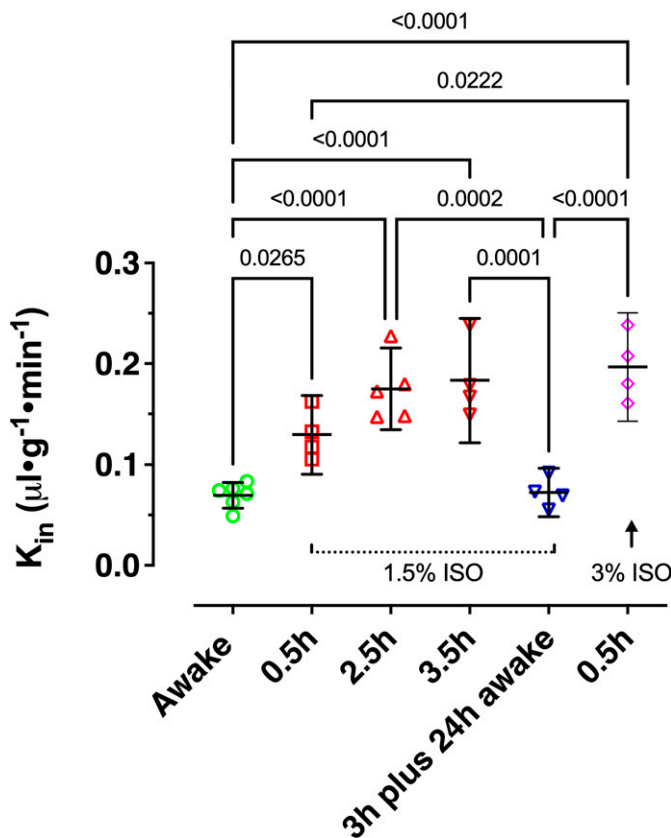
Fig. 5. Brain uptake clearance (K_{in}) in mice measured after different periods or concentrations of isoflurane anesthesia compared with awake mice (i.e., never anesthetized). The awake group received [13C12]sucrose by tail vein injection at time 0. Different subgroups were euthanized at 1, 5, 10, and 20 minutes for blood sampling only. The 30-minute subgroup received [13C6]sucrose as vascular marker at 29.5 minutes via tail vein injection and was euthanized at 30 minutes. In the different anesthesia groups, after induction with 3% isoflurane, animals were kept for the indicated duration under continuous anesthesia with either 1.5% or 3% isoflurane in nitrous oxide/oxygen (70%/30%). For K_{in} measurements [13C12]sucrose was injected intravenously 30 minutes before euthanasia into the jugular vein (i.e., at $t = 0$ for the 0.5-hour group, $t = 2$ hours for the 2.5-hour group, or $t = 3$ hours for the 3.5-hour group). Repeated blood samples were drawn at 1, 5, 10, 20, and 30 minutes after [13C12]sucrose injection. At 29.5 minutes [13C6]sucrose as vascular marker was injected, the 30-minute blood sample was drawn, and animals were euthanized for brain sampling. The 3-hour plus 24-hour awake group was anesthetized for 3 hours under 1.5% isoflurane, allowed to awake, and kept for 24 hours. After 24 hours, the K_{in} of [13C12]sucrose was measured in the awake state as described above. One-way ANOVA, $P < 0.0001$, $n = 4$ to 5 per group for brain sampling. P values for individual group comparisons by Tukey's posttest are provided. The plot depicts individual data, mean, and CI.

agreement with the latter, our ex vivo data did not show any significant changes in the immunofluorescence intensities of the tight junction proteins claudin-5, occludin, and ZO-1 in isoflurane-anesthetized animals versus naïve mice (Fig. 7).

The lack of changes in the tight junction proteins in the face of significant changes in BBB permeability also argues against isoflurane-associated damage to endothelial tight junctions as a cause of increased leakiness. We chose not to probe for potential changes in tight junction protein expression in our human iPSC–derived BMEC model because it has recently been demonstrated that high expression levels and junctional localization of claudin-5, occludin, or ZO-1 can be found in such monolayers despite comparatively poor barrier properties with TEER values in the range of 100 Ω cm^2 (Nishihara et al.,

2020). However, we did not detect any significant changes in TEER values, despite increased permeability of sucrose, in our in vitro transwell system with BMECs even after 6-hour exposure to 3% isoflurane (Fig. 2). TEER is determined by the state of the paracellular tight junctions (Felix et al., 2021), and a decline would be expected if tight junction integrity was compromised. In this respect, our data in iPSC-derived BMEC model differ from the findings by Spieth et al. (2021), who reported decreased TEER values after isoflurane exposure in their in vitro studies in primary murine brain-derived endothelial cell monolayers in monoculture or a coculture system of endothelial cells plus astrocytes and pericytes. It is noteworthy that absolute TEER values in our present study (over 1000 Ω cm^2) were much higher under all conditions compared with basal TEER values of about 100 Ω cm^2 in the endothelial cell (EC) monoculture or about 400 Ω cm^2 in the coculture system of Spieth et al. (2021). If enhanced paracellular passage is excluded, the increased permeability induced by isoflurane should be transcellular. We propose that the demonstrated increase in membrane fluidity also causes an increase of transmembrane permeability of hydrophilic small molecules. The loss of fluorescence dye from EGs preloaded with NaFl in the presence of isoflurane supports that mechanism (Fig. 1, B and C). The EG system reflects pure plasma membrane effects. Lipid domain reorganization as a major cause of increased permeability is well compatible with the rapid time course of permeability changes, which was apparent in vivo as early as about 15 minutes after induction of anesthesia (Fig. 4I) and with reversibility upon removal of isoflurane (Fig. 5).

With respect to the use of NaFl for measurement of passive membrane permeability, there is evidence that it is substrate of membrane transporters of the multidrug resistance-associated protein (MRP), organic anion transporter (OAT), and organic-anion-transporting polypeptides (OATP) families (Sun et al., 2001a,b; Sweet et al., 2002; Hawkins et al., 2007; Patik et al., 2015). This complicates the interpretation of experiments relying on NaFl as a marker of passive BBB permeability. These transporters are energy dependent, either primary or secondary active transporters. Because the EGs used in our present study were suspended in buffer without energy source (ATP or glucose), it is unlikely that any active transmembrane transport could have occurred.

Spieth et al. (2021) postulated a disinhibition of caveolar transcytosis in brain ECs by isoflurane as underlying mechanism of increased barrier permeability. Our data in mice and in EC cultures do not contradict the contribution by such a mechanism. Both caveolae-mediated effects and enhanced diffusibility may coexist and result in increased transmembrane permeability. With respect to the NaFl-loaded EGs, however, a caveolar transport is unlikely. The presence of caveolae in normal red blood cells seems questionable (Leo et al., 2020; Parton et al., 2020) and even if present, in the experimental setup applied here (loss of enclosed dye), an energy-dependent exocytosis step would have been required. There is no source of energy in such EG preparations.

Interestingly, clinical concentrations of both volatile anesthetics, isoflurane and sevoflurane, in the mouse model raised BBB permeability to a similar extent, approximately 2-fold (Fig. 6, D and H). Isoflurane exposure at 1.5% concentration for 3.5 hours increased permeability by 3-fold, and a similar 3-fold increase was observed under 3% isoflurane for 30 minutes (Fig. 5). These significant yet moderate increases are at odds with an up to 180-fold increase in extravasation of NaFl
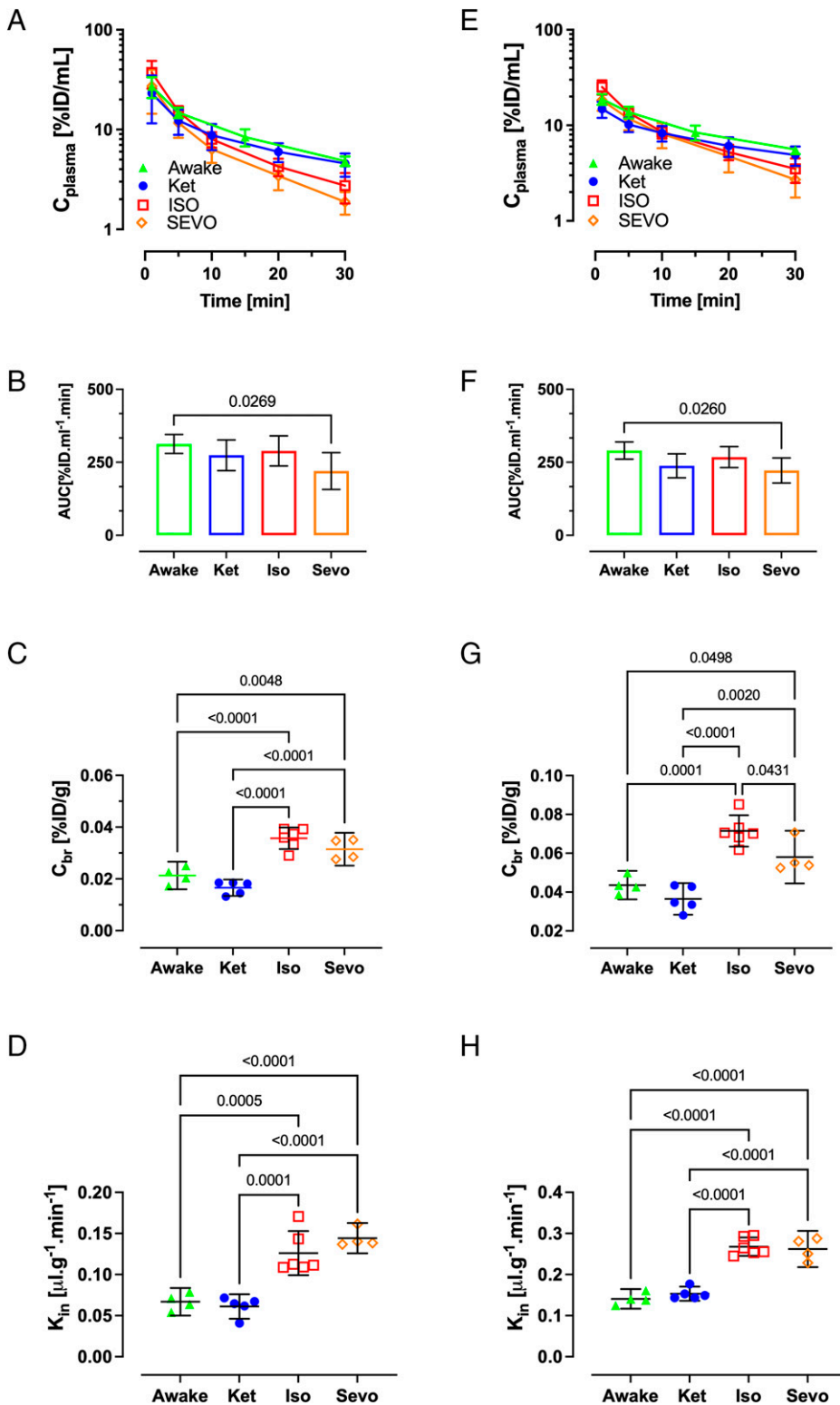
Fig. 6. Plasma profiles and AUC after intravenous bolus injection in mice of [13C12] sucrose (A and B) and [13C6]mannitol (E and F). Injections were performed at time 0 in awake condition or in animals anesthetized with ketamine/xylazine (Ket) (100:10 mg/kg), isoflurane (ISO) 1.5%–2% v/v, or sevoflurane (SEVO) 2%–3% v/v. Brain concentrations were measured in animals euthanized after 30 minutes (depicted in C and G). Apparent K_{in} values for sucrose and mannitol are depicted in (D) and (H), respectively. Graphs show means and CI in (A), (B), (E), and (F) and individual values, means, and CI in (C), (D), (G), and (H). Statistical analysis by one-way ANOVA, $P < 0.001$, $n = 4$–6. P values of individual group comparisons were obtained by Tukey's post-test.

after 3 hours of exposure at 2.5% isoflurane, reported in the study by Spieth et al. (2021). As discussed by the authors, that large increase is a consequence of prolonged exposure to high concentrations of isoflurane, and the mechanism appears unrelated to the effect of lower isoflurane concentrations for shorter time periods on lipid membranes or lipid nanodomains. Although our estimate of apparent K_{in} values of the permeability

markers is based on LC-MS/MS analysis of terminal brain concentrations and the plasma concentration-time course, which provides the input function, Spieth et al. (2021) only compared terminal brain concentrations measured spectrophotometrically, neglecting potential changes to the plasma concentration-time course induced by anesthesia. Nevertheless, the increase in brain uptake of the low molecular weight hydrophilic marker NaFl
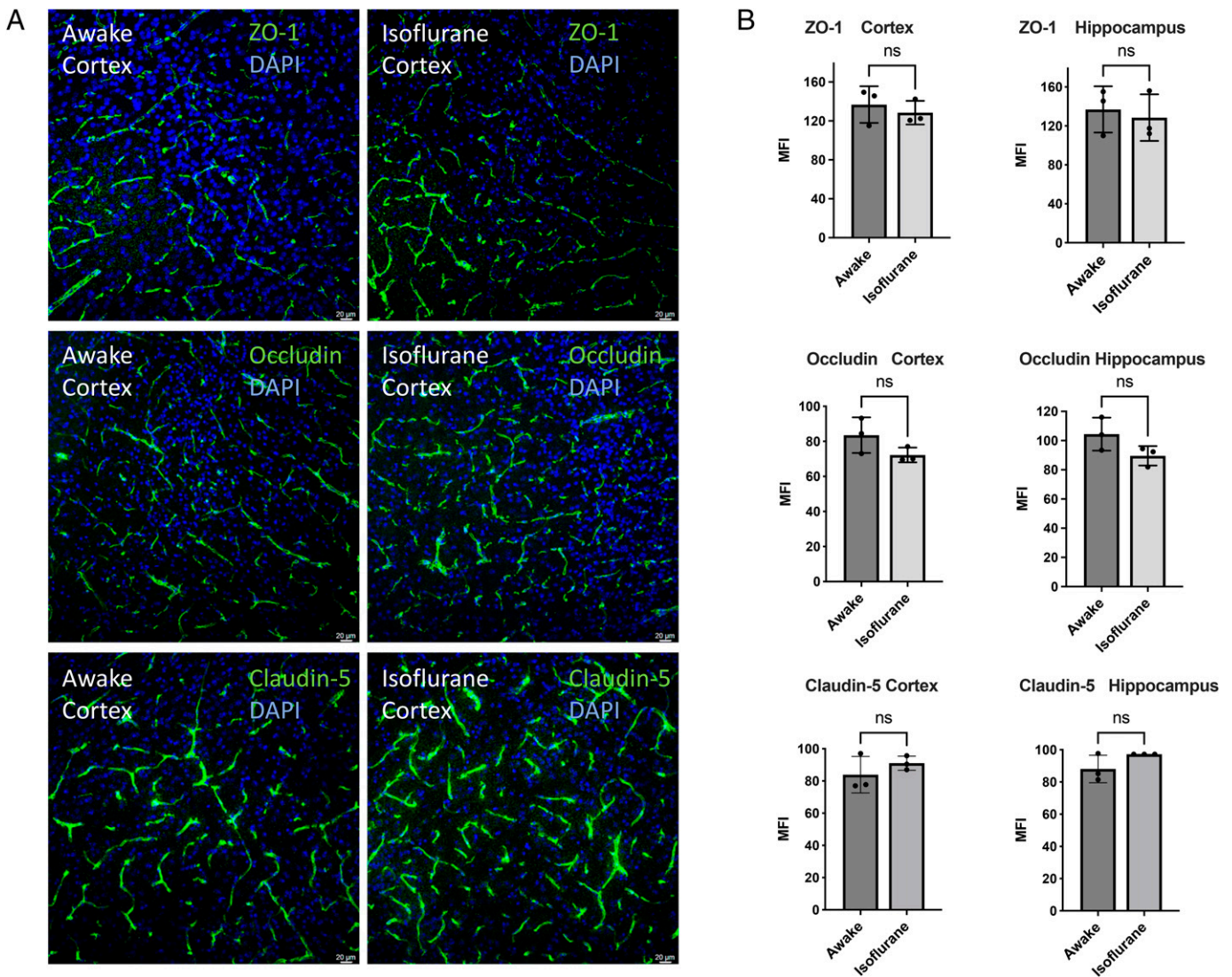
Fig. 7. Representative confocal images of immunofluorescence staining of tight junction proteins on cryosections of brain tissue in the cortical region (A) and quantitative evaluation of mean fluorescence intensity of the capillary profiles in cortex and hippocampus regions (B). Four to five randomly chosen fields from two cortex and two hippocampus sections were analyzed per animal by thresholding and segmentation in Aivia. Unpaired t tests were performed between the isoflurane-treated group and the awake control group ($n = 3$ animals per group).

under short-term exposure (30 minutes) to isoflurane or sevoflurane in their study was in a similar 2- to 3-fold range as the increase in apparent K_{in} of mannitol or sucrose described here.

In contrast to the volatile agents, BBB permeability in our studies with the injectable dissociative anesthetic ketamine, a N-methyl-D-aspartate (NMDA) receptor antagonist, and xylazine, an α_2-adrenergic agonist, was unchanged compared with awake (unanesthetized) mice. Besides the different mechanisms of action between ketamine/xylazine and volatile anesthetics, there is also a large difference in the pharmacologically active concentrations of the volatile anesthetics and ketamine in the body, which may partially explain the absence of a BBB effect by ketamine. Although ketamine plasma concentrations in mice after a 100 mg/kg intraperitoneal dose are in the low micromolar range around 30 μM (Ganguly et al., 2018), the volatile agents are present in blood in millimolar concentration. However, we saw no change in fluorescence anisotropy even at a 367-μM ketamine concentration (Fig. 3).

The 2- to 3-fold increases in the BBB permeability to sucrose and mannitol as a result of in vivo exposure of mice to isoflurane or sevoflurane (Figs. 4I and 5) are much higher than the 25%–40% increases in the permeability of sucrose or sodium fluorescein (Fig. 2A) observed in our in vitro studies with iPSC-derived BBB endothelial cell model. This is not unexpected, as most in vitro models cannot replicate the in vivo conditions both qualitatively and quantitatively. With respect to the iPSC-derived hBMEC model in a transwell setup, as used in the present work, one factor is the absence of shear stress. Among other factors affecting the quality and reproducibility of the model are culture media and supplements used during iPSC expansion and differentiation and the tendency to dedifferentiate from the hBMEC phenotype within a few days in culture. A recent review discusses these challenges (Pervaiz and Al-Ahmad, 2022).

Limitations of the present study include the composition of the anesthesia gases with a nitrous oxide/oxygen (70/30 v/v) content, emulating common clinical practice in humans. Therefore,

the permeability enhancement effect under isoflurane or sevoflurane may include a contribution by nitrous oxide, which could be addressed in future experimental designs. Further, from a translational aspect, the finding of increased BBB permeability in mice may not be quantitatively identical in humans, although there are no compelling published reports suggesting a difference in permeability of endothelial cell membranes between mammalian species.

In conclusion, temporary BBB dysfunction via lipid membrane disturbance by volatile anesthetic agents raises the question of whether it contributes to postoperative delirium, a major clinical problem especially in the elderly patient population (Hughes et al., 2020). The proposed lipid membrane effect could have physiologic and pharmacological ramifications at the BBB. Obviously, permeability would not be increased only for chemicals like sucrose and mannitol but for any low molecular weight hydrophilic substance of endogenous or exogenous origin. For example, brain uptake of hydrophilic drugs with potential neurotoxicity, such as aminoglycosides, should increase under these anesthesia conditions. Conversely, as proposed by Saher's group (Spieth et al., 2021), the enhanced BBB permeability under volatile anesthetics may facilitate drug delivery. Moreover, lipid rearrangement and hence increased cell membrane permeability should affect all cells in the body, not only the endothelial cells at the BBB. This may change the distribution of drugs and endogenous substances with intrinsically low membrane permeability between extracellular and intracellular space, at least for the duration of anesthesia.

Authorship Contributions

Participated in research design: Noorani, Chowdhury, Mehvar, Bickel.

Conducted experiments: Noorani, Chowdhury, Alqahtani, Ahn, Nozohouri, Zoubi, Siddique, Al-Ahmad.

Contributed new reagents or analytic tools: Patel.

Performed data analysis: Noorani, Chowdhury, Alqahtani, Ahn, Wood, Mehvar, Bickel.

Wrote or contributed to the writing of the manuscript: Noorani, Chowdhury, Ahn, Nozohouri, Huang, Mehvar, Bickel.

References

Acharya NK, Goldwaser EL, Forsberg MM, Godsey GA, Johnson CA, Sarkar A, DeMarshall C, Kosciuk MC, Dash JM, Hale CP, et al. (2015) Sevoflurane and isoflurane induce structural changes in brain vascular endothelial cells and increase blood-brain barrier permeability: possible link to postoperative delirium and cognitive decline. *Brain Res* **1620**:29–41.

Akata T, Kanna T, Yoshino J, and Takahashi S (2003) Mechanisms of direct inhibitory action of isoflurane on vascular smooth muscle of mesenteric resistance arteries. *Anesthesiology* **99**:666–677.

Bailer AJ (1988) Testing for the equality of area under the curves when using destructive measurement techniques. *J Pharmacokinet Biopharm* **16**:303–309.

Bedford PD (1955) Adverse cerebral effects of anaesthesia on old people. *Lancet* **269**:259–263.

Belrose JC and Noppens RR (2019) Anesthesiology and cognitive impairment: a narrative review of current clinical literature. *BMC Anesthesiol* **19**:241.

Brown EN, Lydic R, and Schiff ND (2010) General anesthesia, sleep, and coma. *N Engl J Med* **363**:2638–2650.

Chowdhury EA, Alqahtani F, Bhattacharya R, Mehvar R, and Bickel U (2018) Simultaneous UPLC-MS/MS analysis of two stable isotope labeled versions of sucrose in mouse plasma and brain samples as markers of blood-brain barrier permeability and brain vascular space. *J Chromatogr B Analyt Technol Biomed Life Sci* **1073**:19–26.

Doberstein SK, Wiegand G, Machesky LM, and Pollard TD (1995) Fluorescent erythrocyte ghosts as standards for quantitative flow cytometry. *Cytometry* **20**:14–18.

Felix K, Tobias S, Jan H, Nicolas S, and Michael M (2021) Measurements of transepithelial electrical resistance (TEER) are affected by junctional length in immature epithelial monolayers. *Histochem Cell Biol* **156**:609–616.

Ganguly S, Panetta JC, Roberts JK, and Schuetz EG (2018) Ketamine pharmacokinetics and pharmacodynamics are altered by P-glycoprotein and breast cancer resistance protein efflux transporters in mice. *Drug Metab Dispos* **46**:1014–1022.

Hawkins BT and Davis TP (2005) The blood-brain barrier/neurovascular unit in health and disease. *Pharmacol Rev* **57**:173–185.

Hawkins BT, Ocheltree SM, Norwood KM, and Egleton RD (2007) Decreased blood-brain barrier permeability to fluorescein in streptozotocin-treated rats. *Neurosci Lett* **411**:1–5.

Hughes CG, Boncyk CS, Culley DJ, Fleisher LA, Leung JM, McDonagh DL, Gan TJ, McEvoy MD, and Miller TE; Perioperative Quality Initiative (POQI) 6 Workgroup (2020) American Society for Enhanced Recovery and Perioperative Quality Initiative joint consensus statement on postoperative delirium prevention. *Anesth Analg* **130**:1572–1590.

Kadry H, Noorani B, and Cucullo L (2020) A blood-brain barrier overview on structure, function, impairment, and biomarkers of integrity. *Fluids Barriers CNS* **17**:69.

Leo F, Hutzler B, Ruddiman CA, Isakson BE, and Cortese-Krott MM (2020) Cellular microdomains for nitric oxide signaling in endothelium and red blood cells. *Nitric Oxide* **96**:44–53.

Lippmann ES, Al-Ahmad A, Azarin SM, Palecek SP, and Shusta EV (2014) A retinoic acid-enhanced, multicellular human blood-brain barrier model derived from stem cell sources. *Sci Rep* **4**:4160.

Nishihara H, Gastfriend BD, Soldati S, Perriot S, Mathias A, Sano Y, Shimizu F, Gosselet F, Kanda T, Palecek SP, et al. (2020) Advancing human induced pluripotent stem cell-derived blood-brain barrier models for studying immune cell interactions. *FASEB J* **34**:16693–16715.

Noorani B, Chowdhury EA, Alqahtani F, Ahn Y, Patel D, Al-Ahmad A, Mehvar R, and Bickel U (2020) LC-MS/MS-based in vitro and in vivo investigation of blood-brain barrier integrity by simultaneous quantitation of mannitol and sucrose. *Fluids Barriers CNS* **17**:61.

Nozohouri S, Noorani B, Al-Ahmad A, and Abbruscato TJ (2021) Estimating brain permeability using in vitro blood-brain barrier models. *Methods Mol Biol* **2367**:47–72.

Parton RG, Del Pozo MA, Vassilopoulos S, Nabi IR, Le Lay S, Lundmark R, Kenworthy AK, Camus A, Blouin CM, Sessa WC, et al. (2020) Caveolae: the FAQs. *Traffic* **21**:181–185.

Patel J, Chowdhury EA, Noorani B, Bickel U, and Huang J (2020) Isoflurane increases cell membrane fluidity significantly at clinical concentrations. *Biochim Biophys Acta Biomembr* **1862**:183140.

Patik I, Kovacsics D, Német O, Gera M, Várady G, Stieger B, Hagenbuch B, Szakács G, and Özvegy-Laczka C (2015) Functional expression of the 11 human organic anion transporting polypeptides reveals that sodium fluorescein is a general OATP substrate. *Biochem Pharmacol* **98**:649–658.

Pervaiz I and Al-Ahmad AJ (2022) In vitro models of the human blood-brain barrier utilising human induced pluripotent stem cells: opportunities and challenges. *Methods Mol Biol* **2492**:53–72.

Spieth L, Berghoff SA, Stumpf SK, Winchenbach J, Michaelis T, Watanabe T, Gerndt N, Düking T, Hofer S, Ruhwedel T, et al. (2021) Anesthesia triggers drug delivery to experimental glioma in mice by hijacking caveolar transport. *Neurooncol Adv* **3**:vdab140.

Sun H, Johnson DR, Finch RA, Sartorelli AC, Miller DW, and Elmquist WF (2001a) Transport of fluorescein in MDCKII-MRP1 transfected cells and mrp1-knockout mice. *Biochem Biophys Res Commun* **284**:863–869.

Sun H, Miller DW, and Elmquist WF (2001b) Effect of probenecid on fluorescein transport in the central nervous system using in vitro and in vivo models. *Pharm Res* **18**:1542–1549.

Sweet DH, Miller DS, Pritchard JB, Fujiwara Y, Beier DR, and Nigam SK (2002) Impaired organic anion transport in kidney and choroid plexus of organic anion transporter 3 (Oat3 (Slc22a8)) knockout mice. *J Biol Chem* **277**:26934–26943.

Terrando N, Monaco C, Ma D, Foxwell BM, Feldmann M, and Maze M (2010) Tumor necrosis factor-alpha triggers a cytokine cascade yielding postoperative cognitive decline. *Proc Natl Acad Sci USA* **107**:20518–20522.

Tétrault S, Chever O, Sik A, and Amzica F (2008) Opening of the blood-brain barrier during isoflurane anaesthesia. *Eur J Neurosci* **28**:1330–1341.

Thal SC, Luh C, Schaible EV, Timaru-Kast R, Hedrich J, Luhmann HJ, Engelhard K, and Zehendner CM (2012) Volatile anesthetics influence blood-brain barrier integrity by modulation of tight junction protein expression in traumatic brain injury. *PLoS One* **7**:e50752.

Yang S, Gu C, Mandeville ET, Dong Y, Esposito E, Zhang Y, Yang G, Shen Y, Fu X, Lo EH, et al. (2017) Anesthesia and surgery impair blood-brain barrier and cognitive function in mice. *Front Immunol* **8**:902.

Zlokovic BV (2008) The blood-brain barrier in health and chronic neurodegenerative disorders. *Neuron* **57**:178–201.

Address correspondence to: Dr. Ulrich Bickel, Department of Pharmaceutical Sciences, Jerry H. Hodge School of Pharmacy, Texas Tech University Health Sciences Center, 1300 South Coulter Street, Amarillo, TX 79106. E-mail: Ulrich.Bickel@ttuhsc.edu; or Reza Mehvar, Department of Biomedical and Pharmaceutical Sciences, Rinker Health Science Campus, Chapman University, 9401 Jeronimo Road, Irvine, CA 92168. E-mail: Mehvar@chapman.edu